Physics of the Earth and Planetary Interiors, 25 (1981) 129–139
Elsevier Scientific Publishing Company, Amsterdam – Printed in The Netherlands

Mechanism and tectonic implications of the great Banda Sea earthquake of November 4, 1963

Masaki Osada and Katsuyuki Abe

Department of Geophysics, Faculty of Science, Hokkaido University, Sapporo (Japan)

(Received August 27, 1980; accepted for publication October 22, 1980)

Osada, M. and Abe, K., 1981. Mechanism and tectonic implications of the great Banda Sea earthquake of November 4, 1963. Phys. Earth Planet. Inter., 25: 129–139.

The Banda Sea earthquake of November 4, 1963 ($h = 100$ km, $m_B = 7.8$) is probably one of the largest intermediate-depth shocks to have occurred worldwide this century. The mechanism of this earthquake is studied in detail on the basis of P-wave first motion, surface wave and aftershock data. From the analysis of long-period multiple surface waves, a seismic moment of 3.1×10^{28} dyn-cm is obtained, which is the largest reported so far for any intermediate or deep focus shock. This value, together with the estimated fault area of 90×70 km^2, gives an average dislocation of 7.0 m and a stress drop of 120 bar. This event represents an oblique thrust movement on a plane with dip direction N170°E, dip 48° and rake 52°. A geometrical consideration for the fault plane and the configuration of the inclined seismic zone beneath the Banda arc suggests, almost definitely, that the large-scale faulting took place within the subducted plate and offset it. Further repetition of such large-scale faulting might eventually break the subducted plate. The 1963 Banda Sea earthquake thus represents a seismological manifestation of the large-scale deformation of the subducted plate in the mantle.

1. Introduction

The mechanism of great intermediate and deep focus earthquakes provides important clues to the mechanical property and the mode of deformation of subducted plates. In spite of its significance few studies have been made, in contrast with numerous works for great shallow earthquakes. A few examples are the Colombian earthquake of 1970 (Dziewonski and Gilbert, 1974), the South Sandwich earthquake of 1964 (Abe, 1972a), the Brazilian earthquake of 1963 (Fukao, 1972) and the Spanish earthquake of 1954 (Chung and Kanamori, 1976). A major reason for this small number is the infrequent occurrence of great intermediate and deep earthquakes: in addition to this rarity, activity has been very low in recent years in contrast with the high activity in the early years of this century (Abe and Kanamori, 1979).

Since the World-Wide Standard Seismograph Network (WWSSN) was established, the largest deep event in the m_B scale was the intermediate depth earthquake of November 4, 1963, which occurred 100 km beneath the Banda Sea. This earthquake ($m_B = 7.8$) was felt in Australia at Perth and Adelaide, and in New Guinea as far away as Papua. However, little has been known about its focal mechanism and physical size, because its early motions were disturbed by reverberations caused by a relatively small New Hebrides earthquake ($m_B = 6.8$) which occurred about three minutes before. The WWSSN long-period seismograms of the Banda Sea earthquake show very prominent long-period surface waves such as G4 and R4. This large amplitude of long-period waves suggests that this eartquake certainly represents a major tectonic process taking place at intermediate depths beneath the Banda arc. The Banda arc, northwest of Australia, is the eastern continuation of the Sumatra–Java subduction system, which separates the Indian–Australian plate from Eurasia or Southeast Asia (Fitch, 1972; Fitch and Hamil-

0031-9201/81/0000–0000/$02.50

ton, 1974; Cardwell and Isacks, 1978). This paper presents a detailed analysis of seismic data from the 1963 Banda Sea event for the purpose of unraveling its source characteristics and tectonic significance.

2. Seismological data

The hypocenter of the Banda Sea earthquake was redetermined on the basis of P-time data reported in the International Seismological Summary (ISS) and the Bureau Central International Seismologique (BCIS). We used the travel-time table of Jeffreys and Bullen (1958) and all the data for stations in the distance range from 0 to 90° except those whose $O—C$ residual (observed minus computed P time) is more than three times as great as the root-mean-square of all the $O—C$ residuals. The hypocenter parameters thus estimated are: origin time, 01:17:11.4, November 4, 1963; lat., 6.86°S; long., 129.58°E; focal depth, 100 km. The pP data for this event are too poor to constrain the focal depth. The relocated epicenter is shown in Fig. 1, together with other large earthquakes in the Banda arc and eastern Indonesia.

From necessity we also relocated the New Hebrides earthquake which occurred just before the Banda Sea earthquake. The relocated parameters are: origin time, 01:14:29.4, November 4, 1963; lat., 15.06°S; long., 167.40°E; focal depth, 122 km. This focal depth is consistent with eight pP readings reported in ISS which give 126 km. The difference between the New Hebrides and the Banda Sea earthquakes is 2.7 minutes in origin time and 38° in horizontal distance.

The reading of the P-wave first motion on the WWSSN long-period records is difficult because the early portion of the seismogram is severely disturbed by reverberations caused by the New Hebrides earthquake. Eighteen reliable first-motion data could be obtained from the records with the help of travel-time tables. In order to supplement these data, 21 first-motion data reported in ISS were used. All the P-wave data are shown in Fig. 2 on a Wulff grid. The lower half of the focal sphere is projected. Most of the data are compressional, and only two dilatational motions are found, at Guam and Rabaul. In the fault model of earthquakes, the compression and the dilatation fields define two nodal planes which are orthogonal to each other. In the present case the nodal planes cannot be determined uniquely from the P-wave data alone because of the unfavorable distribution of the data. The nodal plane solution will be determined later by combining the P-wave and surface-wave radiation patterns.

For the analysis of surface waves, we mainly used the multiple surface waves G4 (Love waves) and R4 (Rayleigh waves) recorded on the WWSSN long-period seismograms. Other surface waves along the shorter propagation paths could not always be traced because of excessively large amplitudes. The G3 and R3 waves were added wherever possible, in order to obtain as uniform an azimuthal coverage as possible. Using the waveform equalization method described in Kanamori (1970), we equalized the surface waves to a propagation distance of 360° + 270° and a standard 30 s (pendulum period) − 100 s (galvanometer period) instrument with a magnification of 1500. The procedure in practice is described in Abe (1972a). The wave trains thus equalized are shown in Figs. 3 and 4. The circular plots at the centers of these figures show the maximum peak to peak amplitudes on the traces; for the dispersed Rayleigh waves the amplitude of wave trains having group velocities between 3.65 and 3.55 km s^{-1} was measured. The important features of the observed radiation patterns are the lobe pattern, the direction of the lobe and the amplitude ratio of Love to Rayleigh waves. For example, the Love waves indicate a four-lobed radiation pattern, while the Rayleigh wave radiation pattern is two-lobed, and the maximum amplitude of Love waves is much larger than that of Rayleigh waves.

In Figs. 3 and 4 the amplitude of both Love and Rayleigh waves is relatively small in the northeastern quadrant of the radiation patterns. This asymmetry is probably due to the artificial effect of the equalization rather than the effect of a moving source. The region to the southwest of the source is occupied for the most part by the Indian Ocean and the southern Atlantic Ocean where the WWSSN stations are poorly distributed. Owing to this unfavorable coverage of stations, we

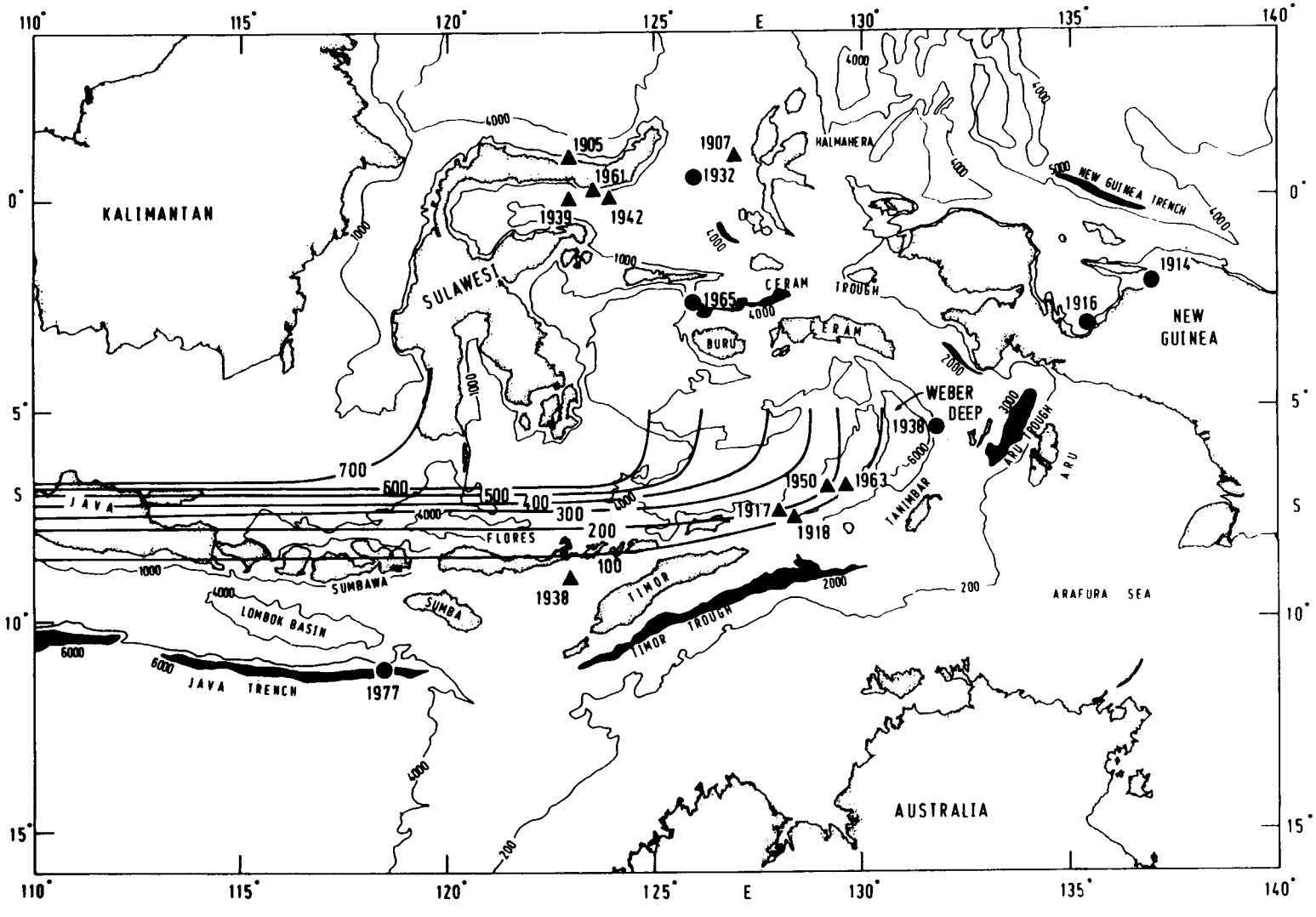

Fig. 1. Map of the Banda arc and eastern Indonesia. Bathymetry (meters) is from Hamilton (1974). The closed circles and triangles show the epicenters of Class *a* shallow earthquakes (Gutenberg and Richter, 1954; Abe and Kanamori, 1980) and deep earthquakes of $m_B \geq 7.5$ (Abe and Kanamori, 1979), respectively. The solid curves are seismic depth contours in kilometers (Cardwell and Isacks, 1978).

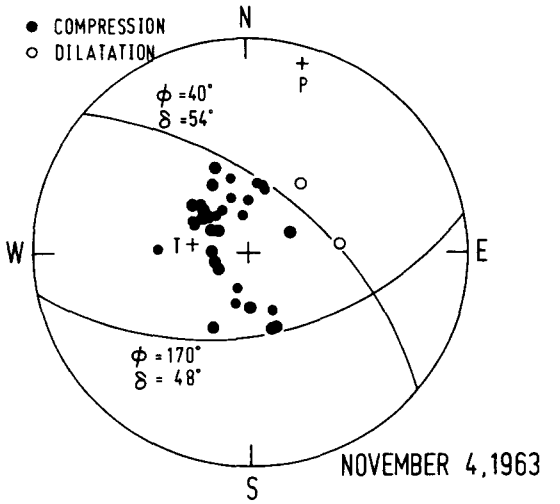

Fig. 2. P-wave first motions for the Banda Sea earthquake. The lower half of the focal sphere is projected on the Wulff grid. Large and small circles are from the WWSSN long-period seismograms and the reports given in ISS, respectively. The nodal planes and P and T axes are also shown.

equalized G3 and R3 to G4 and R4 distances for this particular azimuth. Since this equalization is made for large propagation distances (140° on the average), the validity of the assumed Q values cannot be guaranteed any longer in view of lateral heterogeneity of Q structure (Mills, 1978; Nakanishi, 1979).

The seismograms obtained here can be compared with similar presentations given in Abe (1972a) where another large intermediate depth earthquake ($h = 120$ km) is analyzed. In general, the waveform of Rayleigh waves and the amplitude ratio of Love to Rayleigh waves, at large propagation distances, depend on the source depth (Abe, 1972a). Note that the Rayleigh waves excited by these shocks are, in general, strongly dispersed with a relatively larger amplitude in the earlier part than in the later part. Such waveforms are characteristic of the excitation at an intermediate depth.

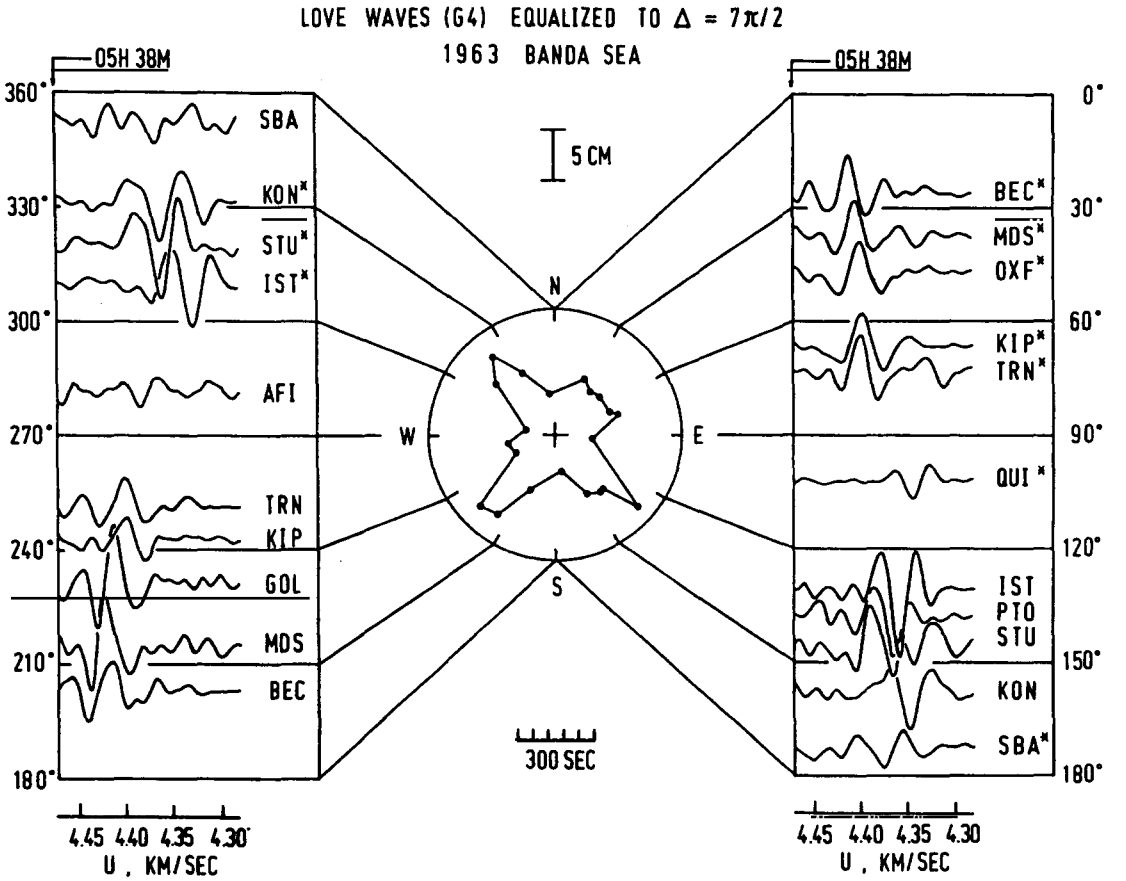

Fig. 3. Love waves (G4) equalized to a propagation distance of $7\pi/2$. Counterclockwise motion around the epicenter is taken upward on the trace. The vertical scale gives the amplitude on the standard 30–100 seismogram with a magnification of 1500. For stations with an asterisk, G3 is equalized to G4 distance. The group velocity scale is given.

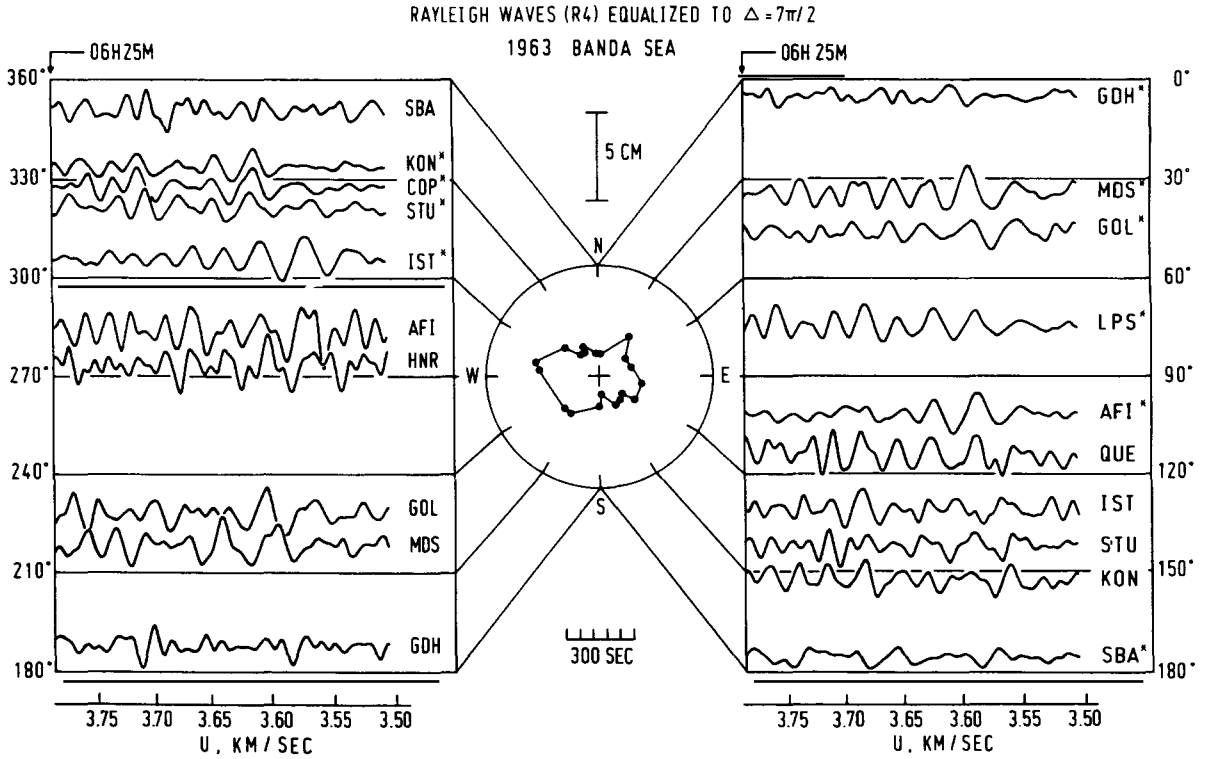

Fig. 4. Rayleigh waves (R4) equalized to a propagation distance of $7\pi/2$. Upward motion is taken upward on the trace. For other explanations, see the caption of Fig. 3.

3. Mechanism

The focal mechanism of the Banda Sea earthquake is determined by combining the P-wave and surface-wave radiation patterns. The synthetic surface waves are computed by the procedure described in Kanamori (1970) and Abe (1972a), and are compared with the observed seismograms for amplitude and radiation pattern. The computation is made for a point source with a step dislocation, located at a depth of 96 km. It is assumed here that the P waves and surface waves originated from a common source.

We first determine the dip direction ϕ and dip angle δ of two nodal planes. These geometrical parameters could not be determined uniquely from the P-wave data alone. However, it is easily found that two dilatational points in Fig. 2 loosely define one nodal plane. The geometry of this plane can be constrained in the range from N40°E to N90°E for ϕ and from 50 to 60° for δ. We will therefore take the following procedure for determining the source geometry. We fix ϕ and δ of one nodal plane within the above range, move the other nodal plane, calculate the synthetic surface waves, and compare them with the observed radiation patterns. This procedure is iterated until good agreement in the radiation patterns for both Love and Rayleigh waves is found. The similar method has been employed in some studies (Kanamori, 1970; Abe, 1973; Stewart and Cohn, 1979). The best fitting solution is that given in Fig. 2: $\phi_1 =$

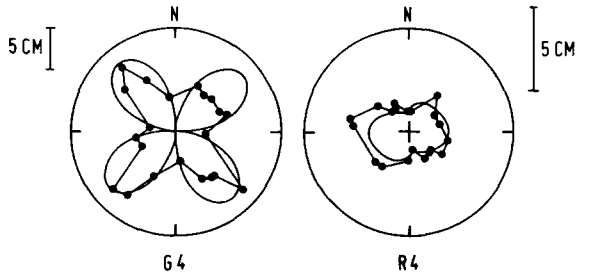

Fig. 5. Comparison of the observed surface-wave radiation patterns with the synthetic patterns. The calculation is made for the source geometry shown in Fig. 2 and $M_0 = 3.1 \times 10^{28}$ dyn-cm. A point source with a step dislocation is located at a depth of 96 km.

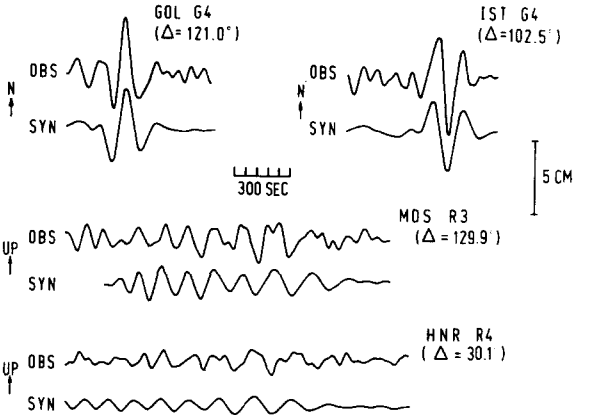

Fig. 6. Comparison between the observed and the synthetic seismograms. The vertical scale gives the amplitude on the standard 30–100 seismogram with a magnification of 1500. The calculation is made for the source geometry shown in Fig. 2 and $M_0 = 3.1 \times 10^{28}$ dyn-cm. A point source with a step dislocation is located at a depth of 96 km.

N170°E and $\delta_1 = 48°$; ϕ_2 = N40°E and $\delta_2 = 54°$. Figure 5 shows the comparison between the observed and synthetic radiation patterns for this solution. Since the present data cannot resolve the details of the radiation patterns, the uncertainty in determining the source geometry is somewhat large, but is not more than 15°. The solution obtained here is found to be very similar to the focal mechanism solution of the nearby earthquakes (Fitch and Molnar, 1970; Cardwell and Isacks, 1978).

From a comparison of the trace amplitudes of the observed and synthetic records, a seismic moment of 3.1×10^{28} dyn-cm is obtained from both Love and Rayleigh waves. In this calculation we did not use the data located in the northeastern quadrant of the radiation patterns for reasons stated before. Some synthetic seismograms calculated for the above source parameters are shown in Fig. 6 in comparison with the observed records. The overall agreement of the waveform is reasonably good.

The actual fault plane can be either a plane dipping 48° to the south or a plane dipping 54° to the northeast. The key to the selection is provided by the spatial distribution of the aftershocks. Figure 7 shows the hypocenters of the aftershocks which occurred within one week after the main shock and one foreshock which occurred at 18:55:38.4 on October 26. All these hypocenters were relocated by using the technique stated earlier. Of nine well-relocated aftershocks, seven occurred within two days after the main shock. Figure 7 clearly indicates that the aftershock zone extends east–west and dips steeply to the south. This leads to the selection of the nodal plane dipping south for the actual fault plane. Thus the Banda Sea earthquake represents a thrust faulting with a left-lateral component (slip angle 52°).

The dimension of the fault plane cannot be determined directly. However, the aftershock area suggests that the fault area has a length of 90 km and downdip width of 70 km. If this value is correct, the average dislocation of the fault D and the stress drop σ are estimated according to the slip dislocation theory of faulting (e.g., Aki, 1972). Using the rigidity of 7×10^{11} dyn cm^{-2}, we have $D = 7.0$ m, $\sigma = 120$ bar (a buried dip-slip fault) and $\sigma = 150$ bar (a circular crack).

4. Tectonic implications

The focal mechanism solution obtained here has the extension axis (T axis) dipping quite steeply and the compression axis (P axis) dipping nearly horizontally (Fig. 2). Such an orientation of the stress axes is characteristic of the intermediate depth earthquakes beneath the Banda arc. Fitch and Molnar (1970), Isacks and Molnar (1971) and

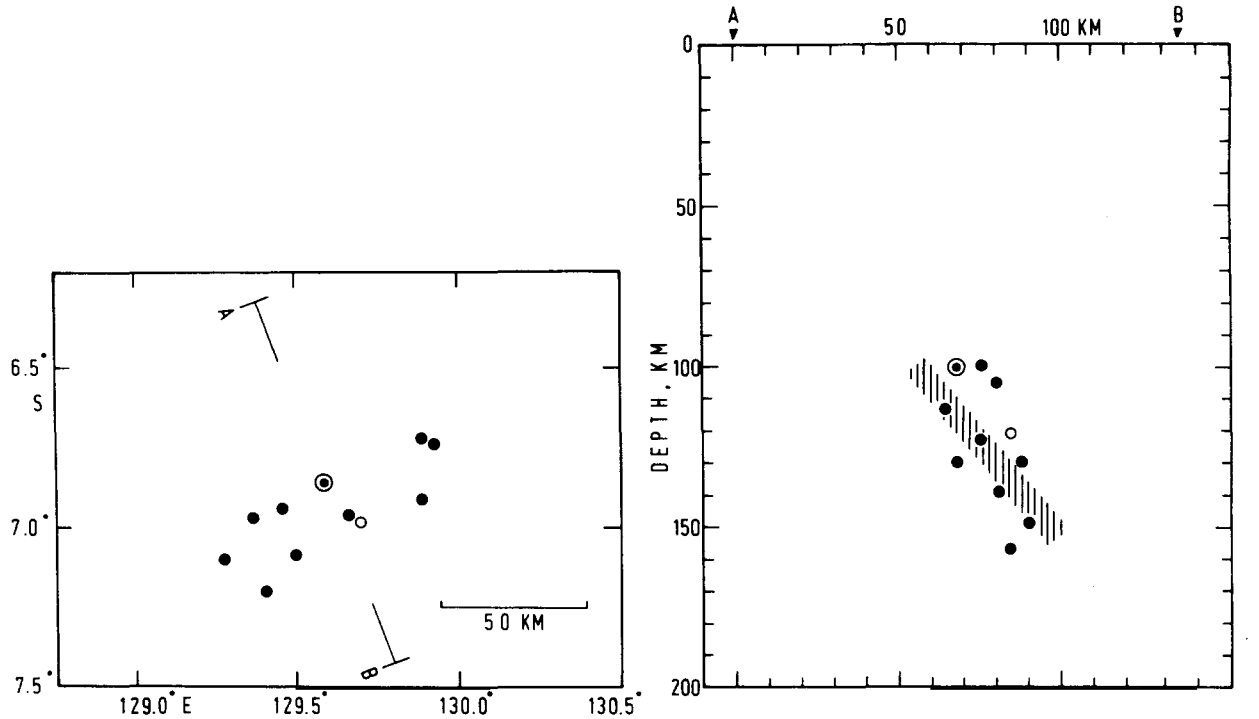

Fig. 7. The spatial distribution of the main shock (double circle), one foreshock (open circle) and aftershocks (closed circle). The vertical cross section is taken along a line AB which is perpendicular to the strike of the fault. The hatched area represents the dip of the fault.

Cardwell and Isacks (1978) have suggested that the downdip extension and the lateral compression result from the gravitational body forces and the lateral bending of the subducted plate, respectively. In the present study we prefer the interpretation that the great Banda Sea earthquake of 1963 represents seismic evidence of a large-scale offset of the subducted plate.

The epicenters of earthquakes in the Banda arc region of 126–132°E are shown in Fig. 8, where events with m_b greater than 5.0 reported in the regional catalogues of the International Seismological Center (ISC) for the years from 1964 through 1976 are plotted. Since these large-magnitude events were, in general, located by large numbers of stations, the quality of the locations is considered fairly good. The vertical cross section of the earthquake hypocenters is shown in Fig. 9. The projection position is taken in accord with section E of Cardwell and Isacks (1978); the azimuth of section EE′ is approximately perpendicular to the local trend of the arc. Figures 8 and 9 show that the seismic activity is markedly intense at intermediate depths, especially in the vicinity of the 1963 Banda Sea event. In Fig. 9, the seismic zone dips to the northwest more steeply at greater depth. The gross configuration of this inclined seismic zone defines the position of the subducted plate in the mantle.

In view of the geometry of the fault plane, its dimension and the gross configuration of the inclined seismic zone, it is suggested, almost definitely, that the 1963 event took place within the subducted plate, at least over the entire thickness of its elastic part. The fault plane of the 1963 event is located by the hatch of region in Fig. 9. The higher seismic activity around the 1963 event is interpreted in terms of the reduced strength in the broken zone.

The fault motion of the 1963 event is not a pure

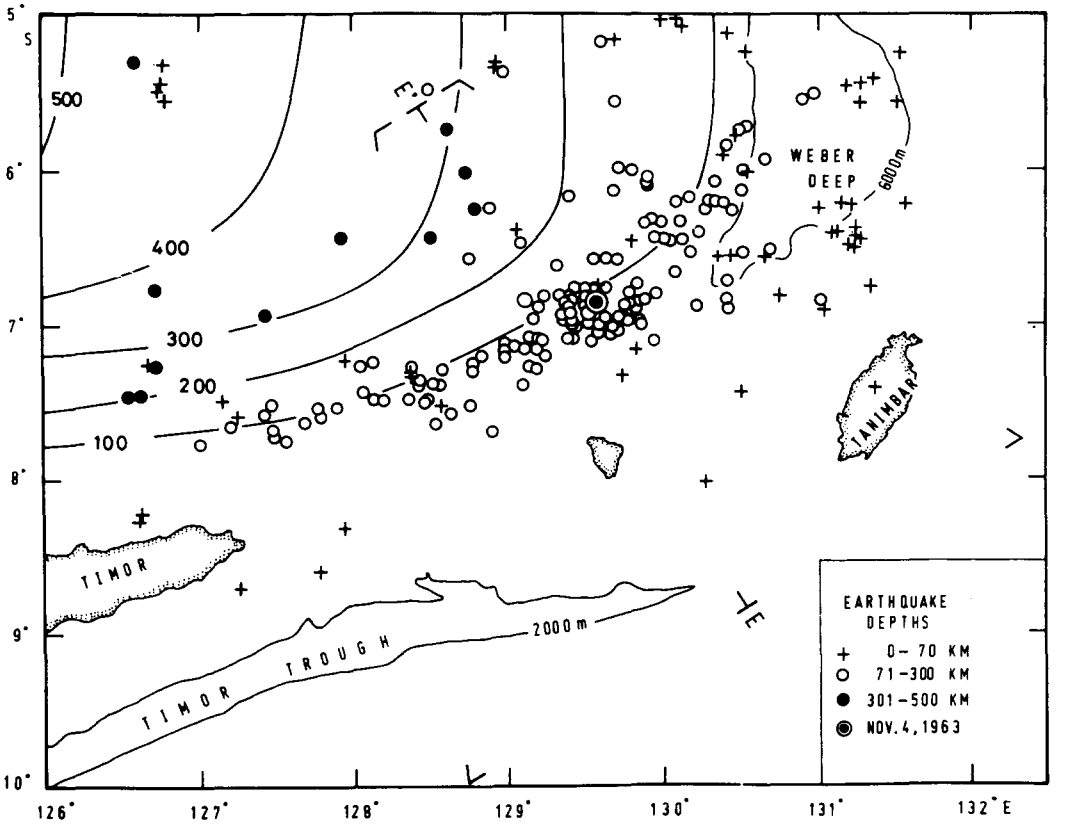

Fig. 8. Seismicity of the Banda arc region. The events are those with m_b greater than 5.0 reported in ISC for the years from 1964 through 1976. The solid curves are seismic depth contours (km) (Cardwell and Isacks, 1978).

dip slip, but an oblique thrust. This oblique motion may result from the lateral bending of the plate. In view of the orientation of the stress distribution in the plate, the tectonic significance of the 1963 event is similar to that of the 1933 Sanriku and the 1970 Peruvian earthquakes which represent large-scale fractures of suboceanic plates due to extensional forces within the plate (Kanamori, 1971; Abe, 1972b).

The 1963 event offset the subducted plate, to a certain extent, at a depth of about 100 km. This movement probably took place on an old fault plane which had once moved, then "healed up". If such an offset is repeated frequently, then it would be expected to accumulate sufficiently to be visible in the configuration of the inclined seismic zone. Figure 9 illustrates our concept of the configuration of the subducted plate in this region, em-

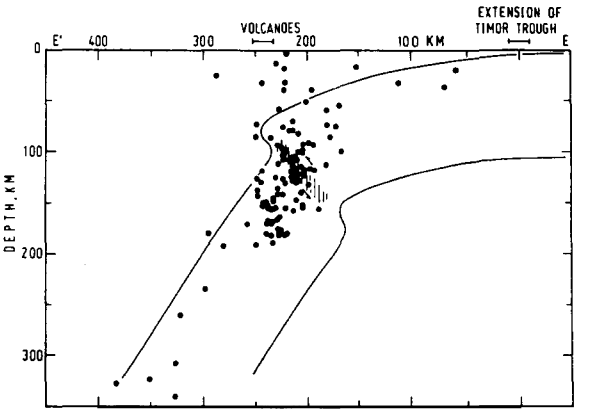

Fig. 9. Vertical cross section of the earthquake hypocenters shown in Fig. 8. The section location is shown in Fig. 8. The proposed configuration of the subducted plate is illustrated schematically (see text). The 1963 Banda Sea event took place along the fault plane shown by the hatch.

phasizing the accumulated offsets of the plate. Though somewhat speculative, the delineation of the plate boundary appears to be consistent with the configuration of the top of the seismic zone, assuming that the suboceanic plate is unlikely to bend sharply at shallow depths.

5. Discussion and conclusion

In this study we have determined the seismic moment of the New Hebrides earthquake for the purpose of estimating its effect on the surface-wave analysis of the Banda Sea event, which it preceded. Using the method described in Kanamori and Stewart (1976), we matched the long-period P-wave record with a synthetic waveform computed for a point double-couple source whose time function was adjusted so that it matched the overall waveform of the first pulse of the P-wave record. A symmetric trapezoidal source time function was used in the synthesis (Kanamori and Stewart, 1976). We also used the fault-plane solution given by Isacks and Molnar (1971). Comparisons of the best synthetics and the observed records are shown in Fig. 10. From the analysis of the P-wave records from nine WWSSN stations, the seismic moment and the rupture process time were estimated to be 1.3×10^{26} dyn-cm and 5 s on average, respectively. This seismic moment is much smaller than that for the Banda Sea event. Thus the excitation of multiple surface waves by the New Hebrides event can be neglected completely in the present analysis.

Of the intermediate depth earthquakes analyzed in detail so far, the largest was the South Sandwich earthquake ($m_B = 7.5$) of May 26, 1964 (Abe, 1972a). This event occurred at a depth of about 120 km near the northern end of the South Sandwich arc, where the north–south trending arc bends sharply toward the west and where seismic activity is markedly intense at intermediate depths (Forsyth, 1975; Frankel and McCann, 1979). This feature is very similar to that in the Banda arc. Moreover, there is a striking similarity between the large South Sandwich shock of 1964 and the Banda Sea shock of 1963, both in the geometry of the nodal planes relative to the trend of the arc and in the magnitude of faulting. The close similarity of both the seismicity and the focal mechanisms of the large shocks in these two regions suggests a similarity in the modes of deformation within the subducted plates. It is very likely that the large-scale offset of the subducted plate, as well as the lateral contortion, is also taking place at an intermediate depth beneath the northern part of the South Sandwich arc.

One of the important parameters obtained in this study is the seismic moment, which represents

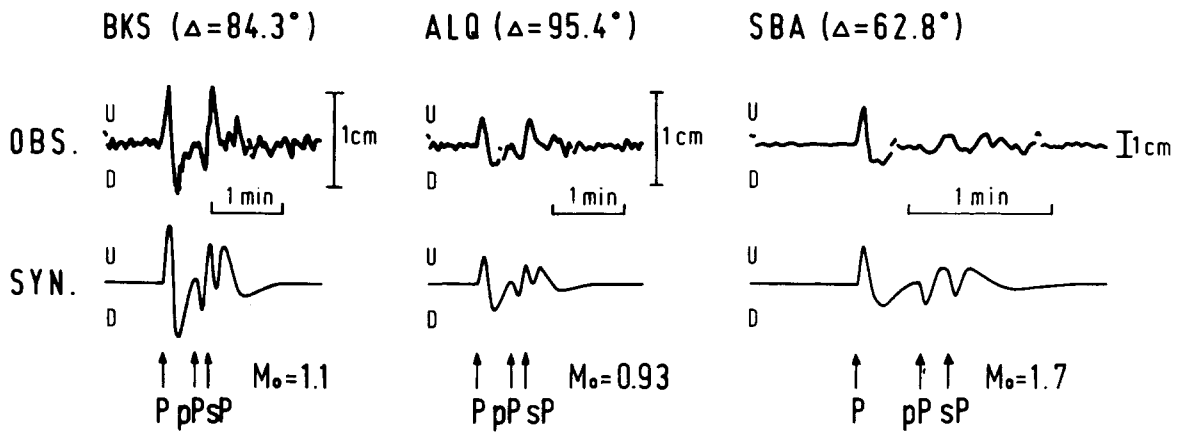

Fig. 10. Observed body waves and matched synthetics for the New Hebrides earthquake of November 4, 1963. The vertical scale gives the amplitude on the standard 30–100 seismogram with a magnification of 1500. The seismic moment M_0 used in the synthetics is given in units of 10^{26} dyn-cm.

the physical size of an earthquake. The seismic moment obtained here, 3.1×10^{28} dyn-cm, is 4.8 times larger than that for the intermediate depth South Sandwich earthquake of 1964 (Abe, 1972a), and 1.3 times as large as that for the deep Colombian earthquake of 1970 (Mendiguren and Aki, 1978). Thus this seismic moment is the largest value reported so far for intermediate and deep focus earthquakes. The stress drop obtained here, 120 bar, is larger than that for great shallow earthquakes (Abe, 1975; Kanamori and Anderson, 1975). This is consistent with the general trend of larger stress drops for deeper earthquakes (Mikumo, 1971; Abe, 1972a; Aki, 1972; Sasatani, 1980). Note that the same stress drop has been obtained for the South Sandwich earthquake of 1964.

A geometrical consideration of the fault plane and the inclined seismic zone suggests, almost definitely, that the great Banda Sea earthquake of 1963 took place within the subducted plate and offset it over the entire thickness of its elastic part. If this faulting had occurred repeatedly in the past, then a large-scale offset of the subducted plate may be expected. Although the expected deformation of the plate is suggested on the configuration of the inclined seismic zone, more precise determinations of earthquake hypocenters in the Banda arc may help to evaluate the above suggestion. With further repetition of such large-scale faulting the subducted plate might be contorted sufficiently to bend very sharply and break off. In discussions of plate tectonics at island arcs, the 1963 Banda Sea earthquake thus gives a crucial clue to the understanding of the mechanism of large-scale deformation of subducted plates in the mantle.

References

Abe, K., 1972a. Focal process of the South Sandwich Islands earthquake of May 26, 1964. Phys. Earth Planet. Inter., 5: 110–122.

Abe, K., 1972b. Mechanisms and tectonic implications of the 1966 and 1970 Peru earthquakes. Phys. Earth Planet. Inter., 5: 367–379.

Abe, K., 1973. Tsunami and mechanism of great earthquakes. Phys. Earth Planet. Inter., 7: 143–153.

Abe, K., 1975. Reliable estimation of the seismic moment of large earthquakes. J. Phys. Earth, 23: 381–390.

Abe, K. and Kanamori, H., 1979. Temporal variation of the activity of intermediate and deep focus earthquakes. J. Geophys. Res., 84: 3589–3595.

Abe, K. and Kanamori, H., 1980. Magnitudes of great shallow earthquakes from 1953 to 1977. Tectonophysics, 62: 191–203.

Aki, K., 1972. Earthquake mechanism. Tectonophysics, 13: 423–446.

Cardwell, R.K. and Isacks, B.L., 1978. Geometry of the subducted lithosphere beneath the Banda Sea in eastern Indonesia from seismicity and fault plane solutions. J. Geophys. Res., 83: 2825–2838.

Chung, W.-Y. and Kanamori, H., 1976. Source process and tectonic implications of the Spanish deep-focus earthquake of March 29, 1954. Phys. Earth Planet. Inter., 13: 85–96.

Dziewonski, A.M. and Gilbert, F., 1974. Temporal variation of the seismic moment tensor and the evidence of precursive compression for two deep earthquakes. Nature (London), 247: 185–188.

Fitch, T.J., 1972. Plate convergence, transcurrent faults, and internal deformation adjacent to southeast Asia and the western Pacific. J. Geophys. Res., 77: 4432–4460.

Fitch, T.J. and Molnar, P., 1970. Focal mechanisms along inclined earthquake zones in the Indonesia–Philippine region. J. Geophys. Res., 75: 1431–1444.

Fitch, T.J. and Hamilton, W., 1974. Reply. J. Geophys. Res., 79: 4982–4985.

Forsyth, D.W., 1975. Fault plane solutions and tectonics of the south Atlantic and Scotia Sea. J. Geophys. Res., 80: 1429–1443.

Frankel, A. and McCann, W., 1979. Moderate and large earthquakes in the South Sandwich arc: indicators of tectonic variation along a subduction zone. J. Geophys. Res., 84: 5571–5577.

Fukao, Y., 1972. Source process of large deep-focus earthquake and its tectonic implications—the western Brazil earthquake of 1963. Phys. Earth Planet. Inter., 5: 61–76.

Gutenberg, B. and Richter, C.F., 1954. Seismicity of the Earth and Associated Phenomena. 2nd edn. Princeton University Press, Princeton, NJ., 310 pp.

Hamilton, W., 1974. Bathymetric map of the Indonesian region. U.S. Geol. Surv., Map I-875-A.

Isacks, B. and Molnar, P., 1971. Distribution of stresses in the descending lithosphere from a global survey of focal-mechanism solutions of mantle earthquakes. Rev. Geophys. Space Phys., 9: 103–174.

Jeffreys, H. and Bullen, K.E., 1958. Seismological Tables. British Association for the Advancement of Science, London, 50 pp.

Kanamori, H., 1970. Synthesis of long-period surface waves and its application to earthquake source studies—Kurile Islands earthquake of October 13, 1963. J. Geophys. Res., 75: 5011–5027.

Kanamori, H., 1971. Seismological evidence for a lithospheric normal faulting—the Sanriku earthquake of 1933. Phys. Earth Planet. Inter., 4: 289–300.

Kanamori, H. and Anderson, D.L., 1975. Theoretical basis of some empirical relations in seismology. Bull. Seismol. Soc. Am., 65: 1073–1095.

Kanamori, H. and Stewart, G.S., 1976. Mode of the strain release along the Gibbs fracture zone, Mid-Atlantic ridge. Phys. Earth Planet. Inter., 11: 312–332.

Mendiguren, J.A. and Aki, K., 1978. Source mechanism of the deep Colombian earthquake of 1970 July 31 from the free oscillation data. Geophys. J.R. Astron. Soc., 55: 539–556.

Mikumo, T., 1971. Source process of deep and intermediate earthquakes as inferred from long-period P and S wave forms, Part 2. J. Phys. Earth, 19: 303–320.

Mills, J.M., Jr., 1978. Great-circle Rayleigh wave attenuation and group velocity, Part IV: regionalization and pure-path models for shear velocity and attenuation. Phys. Earth Planet. Inter., 17: 323–352.

Nakanishi, I., 1979. Phase velocity and Q of mantle Rayleigh waves. Geophys. J.R. Astron. Soc., 58: 35–59.

Sasatani, T., 1980. Source parameters and rupture mechanism of deep-focus earthquakes. J. Fac. Sci. Hokkaido Univ., Ser. 7 (Geophys.), 6: 301–384.

Stewart, G.S. and Cohn, S.N., 1979. The 1976 August 16, Mindanao, Philippine earthquake ($M_s = 7.8$)—evidence for a subduction zone south of Mindanao. Geophys. J.R. Astron. Soc., 57: 51–65.